Long Combination Vehicles Reverse Strategies Based on Articulation Angle Gradient

Citation for the original published paper (version of record):

Ge, Z., Bruzelius, F., Jacobson, B. (2024). Long Combination Vehicles Reverse Strategies Based on Articulation Angle Gradient. Proceedings of the 16th International Symposium on Advanced Vehicle Control: 707-713. http://dx.doi.org/10.1007/978-3-031-70392-8_100

Long Combination Vehicles Reverse Strategies Based on Articulation Angle Gradient

Zhaohui Ge(✉), Fredrik Bruzelius, and Bengt Jacobson

Chalmers University of Technology, 41296 Gothenburg, Sweden
zhaohui.ge@chalmers.se

Abstract. To guide the development of driver assistant systems and fully automated solutions for reversing long combination vehicles (LCVs), the principles for reversing LCVs are investigated using the articulation angle gradient. The widely used *Steady-state Circling Limitation* (SSCL) in reversing LCVs has two main drawbacks: it restricts vehicles from operating with large articulation angles crucial for tight spaces and lacks a well-defined feasible range. Two new reverse principles are introduced that can provide better insight. The first principle extends SSCL to include more extreme articulation angles for single-articulated vehicles. It also addresses the necessity of considering articulation gradients when developing the continuous reverse limitation for multi-articulated vehicles. The second principle introduces limited distance reversing for vehicles that no longer meet the first principle's requirements, providing additional vehicle ending poses useful for tasks like loading and coupling.

Keywords: Combination Vehicle · Kinematic Model · Reverse · Articulation Angle Gradient

1 Introduction

High-capacity transport using multi-articulated LCVs increases efficiency and reduces the emission of the transportation [1]. Reversing those vehicles is a difficult and time-consuming task for drivers [2]. A potential solution to this challenge is developing driver assistant systems or fully automated solutions for reverse tasks.

Matsushita et al. controlled reversing a double-trailer vehicle with a velocity and a trajectory controller [3]. Morales et al. presented a reverse control algorithm that transformed a virtual steering angle at the last trailer into the tractor steering angle and pointed out that their algorithm is feasible only under the condition that none of the articulation angles within the vehicle exceed the corresponding magnitude reached during the vehicle's minimal radius steady-state circling state [4, 5]. That limitation is referred to as the SSCL. Within the SSCL, articulation vehicles are claimed to be able to reverse continuously without any inter-unit clashes. Some research on control algorithms for reversing combination vehicles [6–8] are using paths that follow SSCL for validations. Therefore, SSCL is considered as the basic reverse limitation for LCVs.

The drawbacks of the existing research are that they lack boundaries for their feasible region or that the feasible region is defined incompletely.

G. Mastinu et al. (Eds.): AVEC 2024, LNME, pp. 707–713, 2024.
https://doi.org/10.1007/978-3-031-70392-8_100

2 Kinematic Model

A kinematic vehicle model shown in Fig. 1 is used in this study.

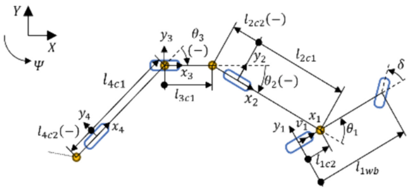

Fig. 1. Vehicle Model

The yaw gradient with respect to the 1st unit's rear axle travel distance is:

$$\frac{\partial \Psi_i}{\partial s_1} = \begin{cases} f_{\frac{\partial \Psi_i}{\partial s_1}}(\delta, \boldsymbol{l_i}), & i = 1 \\ f_{\frac{\partial \Psi_i}{\partial s_1}}(\delta, \boldsymbol{l_i}, \boldsymbol{\theta_{i-1}}), & i = 2, 3, 4, \cdots \end{cases} \tag{1}$$

where Ψ_i is the heading in the global coordinate system, s_1 is the travel distance at the 1st unit's rear axle, δ is the steering angle at the 1st unit's front axle, $\boldsymbol{l_i}$ is the dimensions, as stated in Fig. 1, from the 1st to the i^{th} unit, and $\boldsymbol{\theta_{i-1}}$ is the articulation angle vector of the 1st to the i^{th} articulation angle.

Using Eq. (1), the articulation angle gradient with respect to s_1 is given as:

$$\frac{\partial \theta_i}{\partial s_1} = \frac{\partial \Psi_i}{\partial s_1} - \frac{\partial \Psi_{i+1}}{\partial s_1} = f_{\frac{\partial \theta_i}{\partial s_1}}(\delta, \boldsymbol{l_i}, \boldsymbol{\theta_i}), i = 1, 2, 3, \cdots \tag{2}$$

3 Articulation Angle-Based Reverse Principles Analysis

This section introduces two principles that can be used to develop future reverse strategies. They are established from the articulation angle gradient in Eq. (2) with parameters from several combination vehicles.

As shown in Table 1, the dimensions of nine vehicle combinations [9] are used in the following discussions. Cfg. 1 is a regular tractor and semi-trailer combination. Cfg. 2 to 5 are double-articulated vehicles within 25.25 m limitation. Cfg. 6 to 9 are double- or triple-articulated vehicles within 34.5 m limitation.

All the combinations follow two mechanical constraints. The steering angle δ is limited within $[-45°, 45°]$ [6] and the articulation angles are limited to $[-90°, 90°]$ to avoid inter-unit clashes within the combination.

3.1 Controllable Articulation Angle-Oriented Reverse Principle (CAARP)

For a reversing combination vehicle, it is vital to be able to change the evolution of the articulation angle to avoid inter-unit clashes, which the articulation angles should

Table 1. Vehicle combinations selected for following discussions.

Cfg. No.	1	2	3	4	5	6	7	8	9
Combination in the report [9]	402	602	604	606	705	11	13	1	9

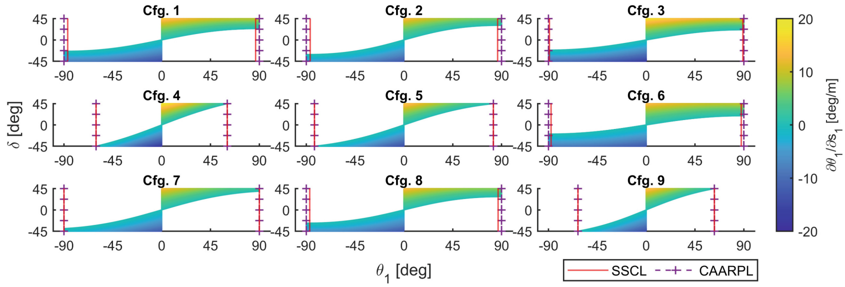

Fig. 2. Comparison between SSCL and CAARPL for single-articulated combinations vehicles.

be able to be controlled to avoid their mechanical limitations. They are called *Controllable Articulation Angles,* a concept introduced in this research. For a single-articulated vehicle, they can be described as:

$$\forall\,|\theta_1| < \theta_{1,CAARP}, \exists\delta \in \left[-45^\circ, 45^\circ\right], \frac{\partial\theta_1}{\partial s_1} \cdot \mathrm{sgn}(s_1) \cdot \theta_1 \le 0 \tag{3}$$

where $\theta_{1,CAARP}$ is the first articulation angle limitation for controllable articulation angle, $\mathrm{sgn}(s_1)$ indicates the travel direction of unit 1.

All the following discussion is based on reversing, which means $\mathrm{sgn}(s_1) = -1$. As shown in Fig. 2, colored zones show the articulation angle gradient that satisfies $\frac{\partial\theta_1}{\partial s_1} \cdot \mathrm{sgn}(s_1) \cdot \theta_1 \le 0$; θ_1 between two red lines are within SSCL; and θ_1 between two purple marked dash lines are feasible for CAARP. The CAARP feasible range is defined as an interval on the one-dimensional articulation angle space.

Equation (3) is satisfied outside the domain described by the SSCL in Cfg. 1, 2, 3, 6 and 8, which indicates CAARP allows for higher articulation angle limitations. This is because these configurations have their rear coupling points on unit 1 in front of their rear axles, and SSCL lacks steady states where the instantaneous rotation center is on different sides of unit 1 and unit 2. For the remaining vehicles, SSCL and CAARP have the same limitation. However, when θ_1 is close to the CAARP limitation, as limited by $\left|\frac{\partial\theta_1}{\partial s_1}\right|$, there will be only limited possibility of reducing the articulation angle. Therefore, one needs to have a margin to this border.

The next step is to extend CAARP to multi-articulated vehicles. To find out how to define the feasible range of CAARP for multi-articulated vehicles, the later part of the statement in Eq. (3) is extended to all articulation angles, and the new statement is given in Eq. (4).

$$\exists\delta \in \left[-45^\circ, 45^\circ\right], \frac{\partial\theta_i}{\partial s_1} \cdot \mathrm{sgn}(s_1) \cdot \theta_i \le 0 (i = 2, 3, \ldots) \tag{4}$$

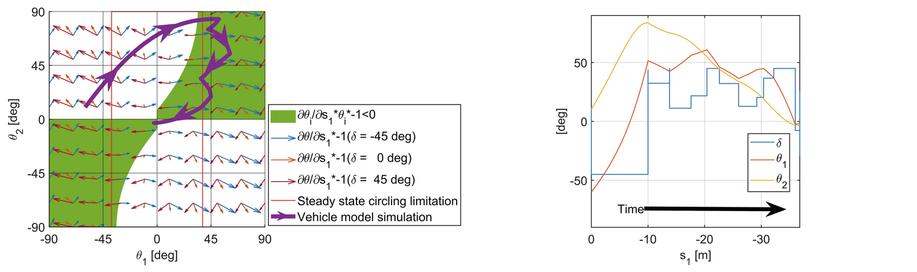

a) Articulation angle trajectory

b) Steering and articulation angles with respect to the travel distance of Unit 1

Fig. 3. Simulation of reverse Cfg. 2 from $\theta_1 = -60°$, $\theta_2 = 10°$ towards a straight pose.

The green areas in Fig. 3a show that the articulation angles satisfy Eq. (4) of a double-articulated vehicle formed with units 1 to 3 of Cfg. 2. Double-articulated combinations formed with the first three units of Cfg. 3 to 9 show similar behaviors. If the same ideal from SSCL is applied, the first part of Eq. (3) should be extended to $\forall|\theta_i| < \theta_{i,lim}$. This should create a rectangular area in Fig. 3a and fully covered by green areas. It is impossible to define such a rectangular in Fig. 3a. This indicates that the CAARP feasible range for multi-articulated vehicles cannot be defined by independently limiting each articulation angle.

Equation (4) is insufficient in defining the feasible range for CAARP of multi-articulated vehicles. Therefore, the articulation angle gradients are considered to further study the feasible range of CAARP. As shown in Fig. 3a, the articulation angle gradient range for a specific pose is expressed by a set of arrows: $\left(-\frac{\partial\theta_1}{\partial s_1}, -\frac{\partial\theta_2}{\partial s_1}\right)_{\delta=-45°,0°,45°}$. For any steering angle within the steering limitation, the articulation angle gradient vector will be within the sector between the arrows for $\delta = -45°$ and $\delta = 45°$ via $\delta = 0°$. This can be proved by the continuity of $\frac{\partial^2\theta_i}{\partial s_1 \partial \delta}$.

As shown in Fig. 3a, the feasible articulation gradient vector plots on the articulation angle plane can offer subjective guidance on whether a vehicle pose is within the CAARP feasible range. For a vehicle pose which is close to the corners of SSCL in the second quadrant, it is impossible to continuously reverse due to all articulation angle vectors in surrounding areas increasing $|\theta_2|$ towards its mechanical limitations. Hence, forward driving is the only possibility before applying CAARP to a vehicle from that pose. We classified long combination vehicles in similar states as NO-NO states, an abbreviation for "if NO forward driving, then NO continuous reversing".

A simulator based on Sect. 2 is built to test the controllability of vehicles' poses outside SSCL. Figure 3 shows one of the simulation results from it. This simulation shows that a pose outside SSCL may still have controllable articulation angles, and articulation angle gradient vectors can guide steering control.

The dimension of the articulation angle space will increase with the number of articulation joints. To describe the articulation gradients of a triple-articulated vehicle, one additional dimension will be added for θ_3, which will turn the 2-D plane in Fig. 3a into a 3-D articulation angle cube. The internal high dimension planning problem, and space constraints are expected to bring additional challenges.

3.2 Locked Articulation Angle-Oriented Reverse Principle (LAARP)

LAARP means the combination vehicle aims for *NO-NO* states, poses outside the CAARP limitation. The *Locked Articulation Angle* appears when at least one articulation angle within a combination vehicle reaches its mechanical limitation, and forward driving is required to avoid clashes. The idea behind LAARP is that the vehicle does not need to reverse further after it arrives at its desired position.

This study shows primary results that show the potential of LAARP. This is done by simulating the combination vehicles with the model from Sect. 2. The vehicle in the simulation will start to reverse with a specific pose, and the steering angle is kept fixed during the reverse. The resolution is 1° for initial articulation angles and 0.1° for the steering angle. The simulation step is given as $\Delta s_1 = 0.1$ m. The simulation ends when the vehicle reaches a locked pose. For a rough estimation, the longer the vehicle can reverse, the greater the potential to manoeuvring the last unit.

Figure 4 shows the maximum reverse distance with fixed steering angles of Cfg. 9, where the position on the articulation angle plane shows the initial pose. Figure 4a and b show the result of a single-articulated vehicle formed by the first two and three units of Cfg.9, respectively. Figure 4c and d show the results of the triple-articulated Cfg.9 that sliced at two different θ_3.

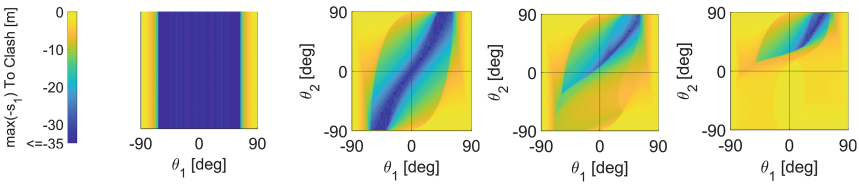

a) Unit 1 to 2 b) Unit 1 to 3 c) Unit 1 to 4 $\theta_3 = 40°$ d) Unit 1 to 4 $\theta_3 = 80°$

Fig. 4. Maximum reverse distances with fixed steering angles of Cfg. 9.

Recall from Fig. 2, the single-articulated vehicle based on Cfg. 9 will no longer satisfy the requirement for CAARP at large articulation angle magnitudes. According to Fig. 4a, the vehicle may still reverse for meters outside CAARP limitations. Figure 4c to d also show non-zero reverse distances appearing in many initial poses of the multi-articulated vehicles, showing the potential outside CAARP feasible range in reverse.

4 Conclusion

This paper investigates principles that can guide the development of reverse strategies for long combination vehicles from the view of kinematical model-based articulation angle gradients. Two principles are established in this paper.

Controllable Articulated Angle-oriented Reverse Principle aims to maintain the vehicles' ability to avoid inter-unit clashes. The feasible range of CAARP can be easily defined by articulation angle limitations for single-articulated vehicles. A more complex limit on each articulation angle dependent on the other articulation angles is necessary for multi-articulated vehicles, which must consider the articulation angle gradients. Analysing the instantaneous kinematics of multi-articulated vehicles of a specific initial pose is insufficient to identify whether the pose is within the feasible range of CAARP. A planning algorithm for vehicle pose change in the articulation angle space is required to define the feasible range for multi-articulated vehicles based on the CAARP.

Locked Articulation Angle-oriented Reverse Principle uses vehicle poses outside the feasible range of CAARP. The preliminary study confirmed the feasibility of LAARP by observing the non-zero reverse distance of the first unit between the nonlocked to locked articulation angle pose.

Compared with the SSCL, the two new reverse principles show possibilities of expanding the feasible vehicle pose ranges for reverse path planning, including additional intermediate poses from CAARP and final poses from LAARP. CAARP excludes certain poses from SSCL intermediate poses for reverse.

References

1. Lindqvist, D., Salman, M., Bergqvist, R.: A cost benefit model for high capacity transport in a comprehensive line-haul network. Eur. Transp. Res. Rev. **12** (2020)
2. Vesmes, A.: Drivers' needs while reversing with a high capacity transport combination. Master's thesis 2023, Chalmers University of Technology (2023)
3. Matsushita, K., Murakami, T.: Backward motion control for articulated vehicles with double trailers considering driver's input. In: IECON Proceedings (Industrial Electronics Conference), pp. 3052–3057 (2006)
4. Morales, J., Martinez, J.L., Mandow, A., Garcia-Cerezo, A.J.: Steering the last trailer as a virtual tractor for reversing vehicles with passive on-and off-axle hitches. IEEE Trans. Ind. Electron. **60**, 5729–5736 (2013)
5. Morales, J., Martínez, J.L., Mandow, A., Medina, I.J.: Virtual steering limitations for reversing an articulated vehicle with off-axle passive trailers. In: IECON Proceedings (Industrial Electronics Conference), pp. 2385–2390 (2009)
6. Rimmer, A.J., Cebon, D.: Planning collision-free trajectories for reversing multiply-articulated vehicles. IEEE Trans. Intell. Transp. Syst. **17**, 1998–2007 (2016)
7. Beglini, M., Lanari, L., Oriolo, G.: Anti-jackknifing control of tractor-trailer vehicles via intrinsically stable MPC. In: Proceedings of the IEEE International Conference on Robot Automation, pp. 8806–8812 (2020)
8. Kusumakar, R.: Autonomous Parking for Articulated Vehicles. HAN University of Applied Sciences (2017)
9. Fröjd, N., Emil, P., Larsson, L.: Svenska HCT Typfordonskombinationer utvärderade mot år 2020 gällande regelverk för BK4 (Swedish HCT Typical Vehicle Combinations Evaluation Based Regulations of Year 2020 for BK4) (2021). https://nvfnorden.org/wp-content/uploads/2021/04/2021-04-15_Svenska_HCT_Typfordon.pdf